Deflection of spacecraft trajectories as a new test of general relativity: Determining the parametrized post-Newtonian parameters β and γ

James M. Longuski,[1] Ephraim Fischbach,[2,*] Daniel J. Scheeres,[3] Giacomo Giampieri,[4] and Ryan S. Park[3]
[1]*School of Aeronautics and Astronautics, Purdue University, West Lafayette, Indiana 47907-1282, USA*
[2]*Department of Physics, Purdue University, West Lafayette, Indiana 47907-1396, USA*
[3]*Department of Aerospace Engineering, The University of Michigan, Ann Arbor, Michigan 48109-2140, USA*
[4]*Space and Atmospheric Physics, Blackett Laboratory, Imperial College, London SW7 28W, England*
(Received 11 July 2003; published 20 February 2004)

In a previous work, we proposed a new test of general relativity (GR) based on a general deflection formula which applies to all values of asymptotic speed V_∞ $(0 \leqslant V_\infty \leqslant 1)$. The formula simplifies to Einstein's light deflection result when $V_\infty = 1$. At low velocity, the general deflection equation reduces to the classical Newtonian contribution along with additional terms which contain the GR effect. A spacecraft, such as the proposed interstellar mission which involves a close pass of the Sun, can be used to exaggerate the GR effect so that it can be accurately measured. In this paper we provide a detailed derivation of the general deflection equation, expressed in terms of the parametrized post-Newtonian constants β and γ. The resulting formula demonstrates that by measuring spacecraft trajectories we can determine β and γ independently. We show via a detailed covariance analysis that β and γ may be determined to a precision of $\sim 4 \times 10^{-5}$ and $\sim 8 \times 10^{-6}$, respectively, using foreseeable improvements in spacecraft tracking.

DOI: 10.1103/PhysRevD.69.042001 PACS number(s): 04.80.Cc, 95.55.Pe

I. INTRODUCTION

In a recent paper [1] a new test of general relativity (GR) was proposed based on the deflection of spacecraft trajectories. One of the new (and unanticipated) features of this test is that in principle it allows the parametrized-post-Newtonian (PPN) parameters β and γ to be disentangled from each other, and hence to be determined separately in a single experiment. In light of Ref. [1], the objectives of the present paper are twofold: (a) to supply the details of the formalism underlying the analysis in Ref. [1] and (b) to explore quantitatively how precisely β and γ can be determined from a specific mission. As part of this discussion we address the question of how well we can determine not only some linear combination of β and γ, such as $(2+2\gamma-\beta)$, but also β and γ separately. As we shall see, the deflection of spacecraft trajectories as a test of GR is of interest not only because of the theoretical possibility of discriminating β and γ, but also because such an experiment appears to be feasible with technology that is either currently available or on the near horizon.

Since the possibility of decoupling β and γ in a single experiment is one of the novel features of the proposed spacecraft mission, it is useful to explain in intuitive terms how this decoupling can come about. The main theoretical result of our analysis is given by the general deflection equation, which is Eq. (8) of Ref. [1] or Eqs. (2.27)–(2.29) in Sec. II of the present paper. We note from Eq. (2.29) that the deflection angle can be expressed as a sum of three contributions, the first of which is purely Newtonian. The sum of this Newtonian contribution and the second term (proportional to γ) yields the GR prediction for light deflection in the limit when the satellite is ultrarelativistic. This is to be expected, since the hyperbolic (open) trajectory of a light ray can be viewed as the limiting case of that for an ultrarelativistic massive object. Finally, the third term in Eq. (2.29) is proportional to the factor $(2+2\gamma-\beta)$, which is also to be expected, since this is the same factor that appears in the GR description of perihelion precession. Thus the two relativistic terms in Eq. (2.29), which are proportional to γ and to $(2+2\gamma-\beta)$, respectively, can be understood as expressing the fact that in some sense a spacecraft in a hyperbolic orbit has characteristics of both a light ray and of a massive object. Finally we note that since the coefficients of γ and $(2+2\gamma-\beta)$ in Eq. (2.29) have a different dependence on the spacecraft velocity, these can in principle be separately determined, thus yielding two independent equations from which β and γ can be inferred.

The preceding discussion leads immediately to the question of whether measuring the gravitational deflection of a spacecraft to the requisite level of precision is technically feasible. It was shown in Ref. [1] that with recent improvements in spacecraft technology, particularly VLBI (very long baseline interferometry) tracking and drag-free systems, a measurement of $(2+2\gamma-\beta)$ to $\sim 10^{-3}$ would be technically feasible in the foreseeable future. In our present work we provide a more detailed covariance analysis which shows that β and γ may be measured to an accuracy of $\sim 4 \times 10^{-5}$ and $\sim 8 \times 10^{-6}$ respectively using advanced *K*-band radiometric tracking.

In Sec. III of the present paper we supply the details of our numerical analysis applied to a specific proposed mission, including a discussion of the contributions from the quadrupole moment of the Sun, J_2. Of particular interest is the question of how well β and γ can be determined *separately* with existing or available technology. Although disentangling β and γ in this (or any other) experiment will be

*Corresponding author.

difficult, the fact that it can be done at all serves to focus attention on strategies for maximizing the sensitivity to the individual parameters. In this connection it is worth noting that improvements in the classic tests of GR have been made possible by the introduction of new technologies, such as the Mössbauer effect and atomic clocks in the case of the gravitational redshift. Additionally, other related tests of GR, including lunar laser ranging [2–4] and tests of both the weak equivalence principle and the gravitational inverse-square law [5], have also benefited from the use of new improvements in technology. Recently [6], improvements in spacecraft tracking techniques applied in the Cassini mission to Saturn have led to a new determination of γ:$(\gamma-1)=(2.1\pm2.3)\times10^{-5}$.

In Sec. IV we develop the theoretical formalism to show how β and γ can be disentangled in a single spacecraft deflection experiment. This formalism characterizes the sensitivity of the trajectory to β and γ, which then leads to the detailed covariance analysis presented in Sec. V. One outcome of this analysis is the recognition that by using the full strength of the range and Doppler radiometric data, highly accurate VLBI measurements become less important. Our results and conclusions are presented in Sec. VI where we consider how standard and advanced tracking accuracies affect the precision to which β and γ can be determined.

II. DERIVATION OF THE GENERAL DEFLECTION EQUATION

To derive the general deflection equation we follow the approach of Longuski et al. [1], but here we take the opportunity to provide additional details. We begin by assuming that a photon or a spacecraft (idealized as a massive particle) approaches a gravitating body from a very great distance (starting with velocity $\mathbf{V}_\infty^-$) and is deflected by gravity. It recedes to a great distance with final velocity $\mathbf{V}_\infty^+$ (see Fig. 1). Let $\phi(r)$ be the angle measured positively (by the right-hand rule) from the inertial direction $\hat{\mathbf{j}}$ to the position vector direction, $\hat{\mathbf{e}}_r$, as shown in Fig. 1. We then define $\phi(r\to\infty)\equiv\phi_\infty$, and also note that $\phi(r_p)=-\pi/2$, where r_p is the distance of closest approach as shown in the figure. From the symmetry between the approach asymptote and the departure asymptote, we can express the total deflection due to gravity, $\Delta\phi_{def}$, as

$$\Delta\phi_{def}=2[\phi_\infty-\phi(r_p)]-\pi. \tag{2.1}$$

We can now make use of the quadrature integral given by Weinberg [7],

$$\phi=\pm\int\frac{A^{1/2}(r)dr}{r^2\{J^{-2}[B^{-1}(r)-E]-r^{-2}\}^{1/2}}, \tag{2.2}$$

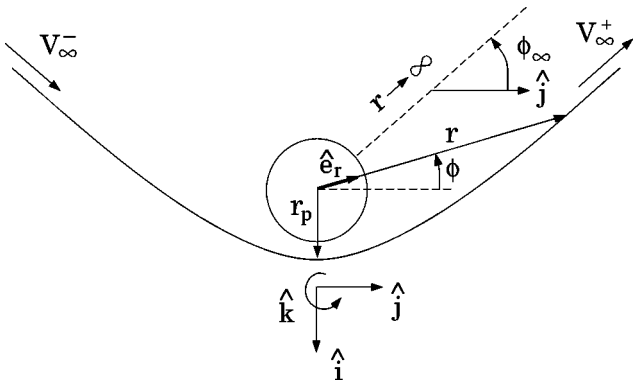

FIG. 1. Deflection of a spacecraft trajectory in a gravity field. The spacecraft approaches with asymptotic velocity $\mathbf{V}_\infty^-$, passes through periapsis (closest approach) at distance r_p, and leaves with asymptotic velocity $\mathbf{V}_\infty^+$. The spacecraft coordinates are given by the radial distance r from the center of the attracting body and the angle ϕ with respect to the inertial direction $\hat{\mathbf{j}}$.

where $A(r)$ and $B(r)$ can be expanded in terms of the constants β and γ of the PPN metric, with $c=1$ [7]:

$$A(r)=1+2\gamma\frac{Gm}{r}+\cdots \tag{2.3}$$

$$B(r)=1-2\frac{Gm}{r}+2\frac{G^2m^2}{r^2}(\beta-\gamma)+\cdots. \tag{2.4}$$

In Eqs. (2.3) and (2.4) G is the Newtonian gravitational constant, m is the mass of the central body, and E and J are constants given by

$$E=1-V_\infty^2, \tag{2.5}$$

$$J=r_p[1/B(r_p)-1+V_\infty^2]^{1/2}. \tag{2.6}$$

Let us now examine the denominator term which appears in Eq. (2.2). Using Eq. (2.5) we have

$$\left\{\frac{1}{J^2}\left[\frac{1}{B(r)}-E\right]-\frac{1}{r^2}\right\}=\frac{1}{J^2}\left[\frac{1}{B(r)}-1+V_\infty^2\right]-\frac{1}{r^2}. \tag{2.7}$$

From Weinberg [7] the inverse of Eq. (2.4) is given by

$$\frac{1}{B(r)}\approx1+\frac{2Gm}{r}+\frac{2G^2m^2}{r^2}(2-\beta+\gamma). \tag{2.8}$$

Upon substituting Eqs. (2.3), (2.7) and (2.8) into Eq. (2.2), we obtain, to order G^2,

$$\phi_\infty-\phi(r_p)=\int_{r_p}^{\infty}\frac{(r^{-1}+\gamma Gmr^{-2})dr}{[V_\infty^2J^{-2}r^2+2GmJ^{-2}r-1+2G^2m^2J^{-2}(2-\beta+\gamma)]^{1/2}}. \tag{2.9}$$

The integrals in Eq. (2.9) can be evaluated using the elementary results [8]

$$\int \frac{dy}{y\sqrt{X}} = \frac{1}{\sqrt{-a}} \sin^{-1}\left(\frac{by+2a}{|y|\sqrt{-q}}\right) \quad (\text{for } a<0), \tag{2.10}$$

$$\int \frac{dy}{y^2\sqrt{X}} = -\frac{\sqrt{X}}{ay} - \frac{b}{2a}\int \frac{dy}{y\sqrt{X}} \quad (\text{for } a\neq 0), \tag{2.11}$$

where

$$X \equiv a + by + cy^2, \tag{2.12}$$

$$q \equiv 4ac - b^2. \tag{2.13}$$

In our problem, Eq. (2.9), we have

$$a = -1 + \frac{2G^2m^2}{J^2}(2-\beta+\gamma),$$

$$b = 2Gm/J^2,$$

$$c = V_\infty^2/J^2,$$

$$q = -\frac{4}{J^2}\left[V_\infty^2 + \frac{G^2m^2}{J^2} - 2V_\infty^2\frac{G^2m^2}{J^2}(2-\beta+\gamma)\right]. \tag{2.14}$$

We evaluate the constants a, b, c, and q by expressing J^2 in terms of r_p and V_∞. From Eqs. (2.6) and (2.8) we obtain

$$J^2 = 2Gmr_p[1 + (Gm/r_p)(2-\beta+\gamma) + r_pV_\infty^2/(2Gm)], \tag{2.15}$$

which gives J^2 in terms of the physically measurable parameters r_p and V_∞. Substituting Eq. (2.15) into Eqs. (2.14) we obtain

$$a = \frac{-1 - r_pV_\infty^2/(2Gm)}{1 + (Gm/r_p)(2-\beta+\gamma) + r_pV_\infty^2/(2Gm)}, \tag{2.16}$$

$$b = \frac{1/r_p}{1 + (Gm/r_p)(2-\beta+\gamma) + r_pV_\infty^2/(2Gm)}, \tag{2.17}$$

$$c = \frac{V_\infty^2/(2Gmr_p)}{1 + (Gm/r_p)(2-\beta+\gamma) + r_pV_\infty^2/(2Gm)}, \tag{2.18}$$

$$q = \frac{-(1/r_p)^2[1 + r_pV_\infty^2/(Gm)]^2}{[1 + (Gm/r_p)(2-\beta+\gamma) + r_pV_\infty^2/(2Gm)]^2}. \tag{2.19}$$

For the expression $1/\sqrt{-a}$ in Eq. (2.10) we write

$$\frac{1}{\sqrt{-a}} = \left[1 + \frac{(Gm/r_p)(2-\beta+\gamma)}{1 + r_pV_\infty^2/(2Gm)}\right]^{1/2}, \tag{2.20}$$

and noting that $Gm/r_p \ll 1$ we have

$$\frac{1}{\sqrt{-a}} \approx 1 + \frac{[Gm/(2r_p)](2-\beta+\gamma)}{1 + r_pV_\infty^2/(2Gm)}. \tag{2.21}$$

Using Eqs. (2.16), (2.17), (2.19), and (2.21) we evaluate the integral of Eq. (2.10) for the upper and lower limits of ∞ and r_p, respectively:

$$\begin{aligned}\int_{r_p}^{\infty} \frac{dy}{y\sqrt{X}} &= \frac{1}{\sqrt{-a}} \sin^{-1}\left(\frac{by+2a}{|y|\sqrt{-q}}\right)\Bigg|_{r_p}^{\infty} \\ &\approx \left\{1 + \frac{[Gm/(2r_p)](2-\beta+\gamma)}{1 + r_pV_\infty^2/(2Gm)}\right\} \\ &\quad \times \left\{\sin^{-1}\left[\frac{1}{1 + r_pV_\infty^2/(Gm)}\right] + \frac{\pi}{2}\right\}.\end{aligned} \tag{2.22}$$

By comparing Eqs. (2.9) and (2.11) we note that the factor $-\gamma Gmb/(2a)$ will appear in the arcsine term [from Eq. (2.10)]; it can be written as

$$\frac{-\gamma Gmb}{2a} = \frac{\gamma Gm/(2r_p)}{[1 + r_pV_\infty^2/(2Gm)]}. \tag{2.23}$$

Collecting all the arcsine terms that result from Eq. (2.9), we obtain

$$\begin{aligned}&\left[1 + \frac{\gamma Gm/(2r_p)}{1 + r_pV_\infty^2/(2Gm)}\right]\left\{1 + \frac{[Gm/(2r_p)](2-\beta+\gamma)}{1 + r_pV_\infty^2/(2Gm)}\right\} \\ &\quad \times \left\{\sin^{-1}\left[\frac{1}{1 + r_pV_\infty^2/(Gm)}\right] + \frac{\pi}{2}\right\} \\ &= \left\{1 + \frac{[Gm/(2r_p)](2-\beta+2\gamma)}{1 + r_pV_\infty^2/(2Gm)}\right\} \\ &\quad \times \left\{\sin^{-1}\left[\frac{1}{1 + r_pV_\infty^2/(Gm)}\right] + \frac{\pi}{2}\right\}.\end{aligned} \tag{2.24}$$

The final term we must analyze from Eqs. (2.9) and (2.11) is

$$
\begin{aligned}
&-\gamma Gm\frac{\sqrt{X}}{ay}\bigg|_{r_p}^{\infty}\\
&\quad=\frac{-\gamma Gm}{a}\sqrt{c}-0\\
&\quad=\frac{\gamma V_\infty (Gm/r_p)^{1/2}}{[2+r_pV_\infty^2/(Gm)]^{1/2}}\left[1+\frac{(2Gm/r_p)(2-\beta+\gamma)}{2+r_pV_\infty^2/(Gm)}\right]^{1/2}\\
&\quad\approx\frac{\gamma V_\infty (Gm/r_p)^{1/2}}{[2+r_pV_\infty^2/(Gm)]^{1/2}}\left[1+\frac{(Gm/r_p)(2-\beta+\gamma)}{2+r_pV_\infty^2/(Gm)}\right],
\end{aligned}
\tag{2.25}
$$

where we note that the value of the function at r_p is zero, and that the final expression is based on the approximation $Gm/r_p \ll 1$.

Equations (2.24) and (2.25) provide the solution to the integral of Eq. (2.9):

$$
\begin{aligned}
\phi_\infty-\phi(r_p)\approx&\frac{\gamma V_\infty (Gm/r_p)^{1/2}}{[2+r_pV_\infty^2/(Gm)]^{1/2}}\\
&\times\left[1+\frac{(Gm/r_p)(2-\beta+\gamma)}{2+r_pV_\infty^2/(Gm)}\right]\\
&+\left\{1+\frac{(Gm/r_p)(2-\beta+2\gamma)}{2+r_pV_\infty^2/(Gm)}\right\}\\
&\times\left\{\sin^{-1}\left[\frac{1}{1+r_pV_\infty^2/(Gm)}\right]+\frac{\pi}{2}\right\}\\
&\text{(for } Gm/r_p\ll 1).
\end{aligned}
\tag{2.26}
$$

To obtain the general deflection equation we write

$$
\begin{aligned}
\Delta\phi_{def}=&2[\phi_\infty-\phi(r_p)]-\pi\\
\cong&2\gamma\epsilon\left(\frac{x}{2+x}\right)^{1/2}+\epsilon\pi\frac{(2+2\gamma-\beta)}{2+x}\\
&+2\left[1+\epsilon\frac{(2+2\gamma-\beta)}{2+x}\right]\sin^{-1}\left(\frac{1}{1+x}\right),
\end{aligned}
\tag{2.27}
$$

where

$$
\epsilon=Gm/r_p\equiv\mu/r_p,\quad x\equiv V_\infty^2/\epsilon,
\tag{2.28}
$$

and where we have retained terms only to order ϵ. It is convenient to rewrite our general deflection equation (2.27) in the final form

$$
\begin{aligned}
\Delta\phi_{def}\cong&2\sin^{-1}\left(\frac{1}{1+x}\right)+2\gamma\epsilon\left(\frac{x}{2+x}\right)^{1/2}\\
&+2\epsilon\frac{(2+2\gamma-\beta)}{2+x}\cos^{-1}\left(\frac{-1}{1+x}\right),
\end{aligned}
\tag{2.29}
$$

where we have used the identity [8] $\pi/2+\sin^{-1}(z)=\cos^{-1}(-z)$. We recognize in Eqs. (2.27)–(2.29) the classical nonrelativistic deflection of a spacecraft trajectory, $\Delta\phi_{NR}$:

$$
\Delta\phi_{NR}\equiv 2\sin^{-1}\left(\frac{1}{1+x}\right).
\tag{2.30}
$$

The nonrelativistic deflection formula is well known to mission designers [9] who use it to compute the effectiveness of the gravity-assist technique, such as that used in the Voyager missions to the outer planets. The $\Delta\phi_{NR}$ term is what remains of Eq. (2.29) when the GR terms (i.e. the ϵ terms) are dropped. We can easily verify Eq. (2.30) by reprising our derivation of Eq. (2.29) with the simplifications

$$
A=1,
\tag{2.31}
$$

$$
B(r)=1-2\frac{Gm}{r}.
\tag{2.32}
$$

The result of these weak field approximations is that we obtain the Newtonian deflection. In this particular derivation the second term of the numerator in the integrand of Eq. (2.9), γGmr^{-2}, vanishes so that only terms corresponding to Eq. (2.10) remain. An immediate consequence of the weak field assumption is that the term $(2-\beta+\gamma)$ which appears in the constants a and q of Eq. (2.14) also vanishes, and hence all terms containing β and γ are eliminated from Eq. (2.26). Since these are directly associated with $\epsilon\equiv Gm/r_p$, we merely drop the ϵ terms which appear explicitly in Eq. (2.30) to obtain the Newtonian deflection formula, Eq. (2.30). Equation (2.30) gives the total turn angle of the vector $\mathbf{V}_\infty$ (i.e., the angle between the approach velocity, $\mathbf{V}_\infty^-$, and the departure velocity, $\mathbf{V}_\infty^+$) based on Newton's law of gravity. If we substitute $V_\infty=1$, or $x=1/\epsilon$, into Eq. (2.30), we obtain the deflection of light predicted by Newtonian physics:

$$
\Delta\phi_{NR}\left(\frac{1}{\epsilon}\right)\cong 2\epsilon.
\tag{2.33}
$$

Similarly, setting $V_\infty=1$ in Eq. (2.29) yields

$$
\Delta\phi_{def}\left(\frac{1}{\epsilon}\right)=2\epsilon(1+\gamma)=\frac{4Gm}{r_p}\left(\frac{1+\gamma}{2}\right),
\tag{2.34}
$$

where terms $O(\epsilon^2)$ and higher have been dropped. Equation (2.34) yields Einstein's formula for the deflection of light when γ is set to unity: twice the value given by Eq. (2.33).

We note that Eq. (2.29) contains the same factor that appears in the formula for the precession of perhelia [7],

$$
\Delta\phi_{prec}=\frac{6\pi Gm}{L}\left(\frac{2+2\gamma-\beta}{3}\right),
\tag{2.35}
$$

where $\Delta\phi_{prec}$ is the precession in radians per revolution, and L is the semilatus rectum of the elliptical orbit. What is remarkable about the factor $(2+2\gamma-\beta)$ in the general deflection equation (2.29) is that the contribution from this term depends on the speed x. This means that an experiment based

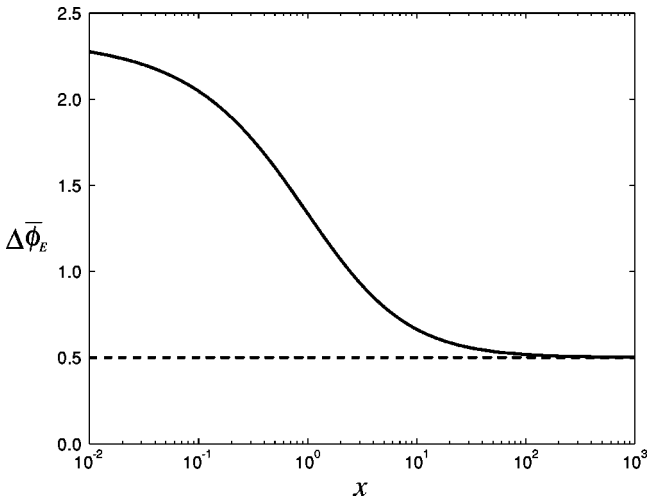

FIG. 2. Plot of the function $\Delta\bar{\phi}_E$ in Eq. (2.37). As discussed in the text, $\Delta\bar{\phi}_E$ gives the scaled contribution of GR to the deflection, plotted versus the scaled speed x. For an incident light ray $\Delta\bar{\phi}_E = 1/2$.

on the deflection equation can discriminate between the contributions from β and γ by comparison to the precession of Mercury's orbit. It is thus clear that at different speeds, an experiment based on the general deflection equation can separately determine the values of β and γ. This is not true for other experiments, such as light deflection, radar time delay, or planetary precession.

We wish to obtain a formula that conveniently compares the general relativistic effect on spacecraft deflection to light deflection. One way to proceed is to define a quantity $\Delta\bar{\phi}$ obtained by subtracting the (often large) angle $\Delta\phi_{NR}$ in Eq. (2.30) from the expression in Eq. (2.29), and to then normalize the result (i.e. divide) by the GR result $2\epsilon(1+\gamma)$:

$$\Delta\bar{\phi} \equiv (\Delta\phi_{def} - \Delta\phi_{NR})/[2\epsilon(1+\gamma)]$$
$$= [\gamma/(1+\gamma)][x/(2+x)]^{1/2} + (1+\gamma)^{-1} \times [(2+2\gamma-\beta)/(2+x)]\cos^{-1}[-1/(1+x)]. \tag{2.36}$$

For Einstein's theory, $\beta = \gamma = 1$ and Eq. (2.36) becomes

$$\Delta\bar{\phi}_E = \frac{\Delta\phi_E}{2\epsilon(1+\gamma)} = \frac{1}{2}\left(\frac{x}{2+x}\right)^{1/2} + \frac{(3/2)}{(2+x)}\cos^{-1}\left(\frac{-1}{1+x}\right). \tag{2.37}$$

The function $\Delta\bar{\phi}_E$ is plotted in Fig. 2. We note from Eq. (2.37) that when $V_\infty = 1$, then $\Delta\bar{\phi}_E \cong 0.5$, as expected: the ratio of the purely relativistic bending of light divided by the total bending of light (including the Newtonian bending) is 1/2. In contrast, for a parabolic trajectory $V_\infty = 0$ (i.e. $x = 0$) and $\Delta\bar{\phi}_E(0) = 3\pi/4 = 2.36$. When $x = 1$, then $V_\infty = \sqrt{Gm/r_p}$ which is the circular speed at a radius r_p. Thus the x variable is conveniently scaled in terms of "circular speeds" at r_p. For $x = 1$, $\Delta\bar{\phi}_E = 1.34$. We see that there are many cases where the relativistic deflection of a spacecraft trajectory is greater than the deflection of light for the same periapsis distance, r_p, where periapsis is the point of closest approach. The question to be answered is whether an experiment can be devised to measure this effect.

TABLE I. Representative values for spacecraft deflections.

Parameter	Earth	Jupiter	Sun
r_p [km]	6678	71 700	2.784×10^{6}
V_∞ [km/s]	9.000	5.455	37.92
Gm [km]	4.435×10^{-6}	1.410×10^{-3}	1.476
ϵ	6.641×10^{-10}	1.966×10^{-8}	5.303×10^{-7}
x	1.357	1.684×10^{-2}	3.017×10^{-2}
$\Delta\phi_{NR}$ [deg]	50.21	159.1	152.2
$\Delta\phi_E$ [rad]	3.229×10^{-9}	1.767×10^{-7}	4.673×10^{-6}
$\sigma_{\Delta r_p}$ [km] [a]	2.156×10^{-8}	1.267×10^{-5}	1.300×10^{-2}

[a]Approximate error tolerance on periapsis knowledge to obtain β and γ to 10^{-3}.

In Table I we estimate the total deflection angle $\Delta\phi_{def}$ [from Eq. (2.27)] and the deflection angle due to GR, $\Delta\phi_E$ [found by multiplying Eq. (2.36) by $2\epsilon(1+\gamma)$], for representative hyperbolic spacecraft trajectories near the Earth, Jupiter, or the Sun. For these calculations we assume that $\beta = \gamma = 1$. In anticipation of the more detailed analysis presented in Secs. IV and V below, we estimate the accuracy required to measure the relativistic deflection, $\Delta\phi_E$, to within 0.1% (the level of sensitivity necessary to determine β and γ to 10^{-3}). For purposes of this estimate we use the approximation [1] [see Eq. (3.10)] $\sigma_{\Delta r_p} = 0.1\%\Delta\phi_E r_p$, which sets a limit on the closest approach distance, r_p. (Other variables affect the sensitivity, but knowledge of r_p is the dominant error source.) Clearly the level of accuracy required to perform the experiment with spacecraft deflections at Earth or Jupiter is beyond present day technology, because periapsis must be known to within 21.56 μm or 1.267 cm, respectively. Since we evidently require a larger gravitational parameter, Gm, we turn our attention to the Sun—the largest gravitating body at our disposal.

III. PROPOSED EXPERIMENT

Mewaldt et al. [10] have proposed the Small Interstellar Probe mission which would cross the solar wind termination shock and heliopause and penetrate into nearby interstellar space. In order to accomplish its scientific objectives, the probe must attain $V_\infty \approx 1.3\times10^{-4}$. To achieve this speed a number of gravity assist scenarios are suggested [10], most of which involve a final close flyby of the Sun at 4 solar radii ($4r_\odot$). At perihelion a maneuver is performed to change the speed of the spacecraft by several km/s in order to send the probe off on its hyperbolic trajectory. The Interstellar Probe mission presents an ideal trajectory to observe the relativistic deflection, provided that the effects of non-gravitational forces and the Newtonian deflection can be accounted for. We will therefore use this mission as the basis for some simple numerical estimates. In Secs. IV and V we present a

more detailed analysis of such a mission and its ability to disentangle the PPN parameters β and γ.

Let us first estimate how accurately the relevant parameters must be known in order to discriminate between the relativistic and Newtonian deflections. Using $r_p = 4 \times 6.960 \times 10^5$ km $= 2.784 \times 10^6$ km, and $Gm = 1.476$ km, we find $\epsilon = 5.303 \times 10^{-7}$ and $x = 3.017 \times 10^{-2}$. Inserting these values of ϵ and x into Eq. (2.37), and multiplying by 4ϵ gives the total general relativistic deflection $\Delta\phi_E = 4.673 \times 10^{-6}$ rad $= 0.9639''$. On the other hand, the nonrelativistic Newtonian deflection is, from Eq. (2.30), $\Delta\phi_{NR} = 2.656$ rad $= 152.2°$, which is very large compared to the relativistic deflection. Thus in order to observe the relativistic deflection we must have very precise knowledge of the Newtonian contribution. (Of course in the case of the Interstellar Probe we will only observe the departure asymptote, namely half the deflections given by $\Delta\phi_E$ and $\Delta\phi_{NR}$.) We proceed to assess our ability to measure the relativistic effect, which will be proportional to the knowledge errors in the nonrelativistic effect.

We can view the rotation induced by general relativity on a hyperbolic trajectory as being a shift in the argument of periapsis of the probe trajectory due to the gravitational interaction, analogous to the advance in Mercury's perihelion. Thus, in order to determine if this is a measurable effect, we must devise a series of ideal measurements to estimate the shift in argument of periapsis between perihelion and escape. At perihelion the argument of periapsis is related to the unit vector of the probe (assuming orbit plane coordinates) by the equation

$$\hat{\mathbf{r}}_p = \cos(\omega)\hat{\mathbf{i}} + \sin(\omega)\hat{\mathbf{j}}, \tag{3.1}$$

where ω is the argument of periapsis (arbitrarily set to zero in Fig. 1) and $\hat{\mathbf{i}}$ and $\hat{\mathbf{j}}$ are unit vectors of our coordinate frame, with the third unit vector $\hat{\mathbf{k}} = \hat{\mathbf{i}} \times \hat{\mathbf{j}}$. When the probe is sufficiently far from the Sun on its escape trajectory, its asymptote can similarly be specified by the unit vector

$$\hat{\mathbf{r}}_\infty = \cos(\omega' + \theta_\infty)\hat{\mathbf{i}} + \sin(\omega' + \theta_\infty)\hat{\mathbf{j}}, \tag{3.2}$$

where ω' is the new (shifted) argument of periapsis, and θ_∞ is the limiting value of the true anomaly of the probe as it escapes from the Sun. In principle, each of these unit vectors can be measured, and the shift in argument of periapsis can be computed by comparing them. Specifically,

$$|\hat{\mathbf{r}}_p \times \hat{\mathbf{r}}_\infty| = \sin(\omega' - \omega)\cos\theta_\infty + \cos(\omega' - \omega)\sin\theta_\infty, \tag{3.3}$$

and we define $\omega' - \omega \equiv \Delta\phi$, which is the quantity we wish to measure. Noting that $\Delta\phi \ll 1$, $\cos\theta_\infty = -1/e$, and $\sin\theta_\infty = \sqrt{e^2 - 1}/e$, where e is the eccentricity, we can solve for $\Delta\phi$ in terms of measurable quantities:

$$\Delta\phi = \sqrt{e^2 - 1} - e|\hat{\mathbf{r}}_p \times \hat{\mathbf{r}}_\infty|. \tag{3.4}$$

We next take the variation (δ) of the measurement, Eq. (3.4), to compute how errors in measuring the eccentricity and the unit vectors will contribute to errors in the measured value of $\Delta\phi$:

$$\delta\Delta\phi = [e(e^2 - 1)^{-1/2} - |\hat{\mathbf{r}}_p \times \hat{\mathbf{r}}_\infty|]\,\delta e - e\,\delta|\hat{\mathbf{r}}_p \times \hat{\mathbf{r}}_\infty|. \tag{3.5}$$

Noting that $|\hat{\mathbf{r}}_p \times \hat{\mathbf{r}}_\infty| \cong \sqrt{e^2 - 1}/e$ reduces Eq. (3.5) to

$$\delta\Delta\phi = e^{-1}(e^2 - 1)^{-1/2}\delta e - e[(\hat{\mathbf{k}} \times \hat{\mathbf{r}}_p) \cdot \delta\hat{\mathbf{r}}_\infty + (\hat{\mathbf{r}}_\infty \times \hat{\mathbf{k}}) \cdot \delta\hat{\mathbf{r}}_p], \tag{3.6}$$

which represents the effect of variations in the angular position of the probe at periapsis and at escape. Careful evaluation of each term for a general flyby shows that the expression in square brackets in Eq. (3.6) can be expressed as

$$e[\cdots] = e\,\delta|\hat{\mathbf{r}}_p \times \hat{\mathbf{r}}_\infty| = \Delta r_\infty / r_\infty + \Delta r_p / r_p, \tag{3.7}$$

where Δ denotes errors in distance measured normal to the radius vector. Since the eccentricity is, in turn, a function of specific measurable quantities via the relation $e = [1 + (r_p V_\infty^2/\mu)]$, we have

$$\delta e = (e - 1)[\delta r_p / r_p + 2\,\delta V_\infty / V_\infty - \delta\mu/\mu], \tag{3.8}$$

where δr_p denotes variations along the radius vector. If we combine the previous results and assume that the different measurements are uncorrelated, then the overall uncertainty in $\Delta\phi$ is

$$\sigma_{\Delta\phi}^2 = e^{-2}[(e-1)/(e+1)][(\sigma_{r_p}/r_p)^2 + 4(\sigma_{V_\infty}/V_\infty)^2 + (\sigma_\mu/\mu^2)] + [(\sigma_{\Delta r_p}/r_p)^2 + (\sigma_{\Delta r_\infty}/r_\infty)^2], \tag{3.9}$$

where σ denotes the Gaussian standard deviation of the measured quantity.

In general, the uncertainties in the first terms will be negligible compared to the measured uncertainties $\sigma_{\Delta r_p}$ and $\sigma_{\Delta r_\infty}$. Additionally, at escape the probe unit vector direction can be measured extremely accurately using established VLBI techniques [11]. This leaves the down-track measurement of the probe position at perihelion as the dominant error source, so that

$$\sigma_{\Delta\phi} \approx \sigma_{\Delta r_p}/r_p. \tag{3.10}$$

Current navigation practice would reduce $\sigma_{\Delta r_p}$ to the order of 1–10 km [12]. Taking $\sigma_{\Delta r_p} = 1$ km for our numerical example (where e is computed to be 1.03), we find that $\sigma_{\Delta\phi} = 3.6 \times 10^{-7}$ rad which, by comparison to half the deflection angle $\Delta\phi_E$, represents an error of 16%. If this measurement

uncertainty were reduced to the order of 10 m, then we would estimate that the contribution from the PPN parameters β and γ could be found to 10^{-3}. Measurement uncertainties of this order imply Earth-based measurement accuracies on the order of 0.1 nrad. Based on operationally demonstrated measurements of the Deep Space Network's VLBI system, its estimated accuracy at present is of order 5 nrad. Observations of natural radio sources made with the VLBI measurement technique have demonstrated accuracies of 0.8 nrad, and the fundamental limit on such measurements is of order 0.01 nrad [13]. This precision is substantially better than the 0.1 nrad accuracy required to measure β and γ at the $\sim 10^{-3}$ level. The feasibility of developing this technology to the levels of accuracy needed for our proposed experiment and for near-Sun observations is considered in Ref. [14]. We can presume that the increases in accuracy of VLBI will be accompanied by corresponding improvements in the infrastructure needed to support these measurements, which would likely be developed in concert with improved VLBI technology.

An important perturbation not directly addressed here is due to the J_2 gravity coefficient of the Sun. The shift induced in periapsis due to this will be on the order of 1% of the shift induced by general relativity. Thus, it will introduce additional errors in the determination of β and γ. In order to discriminate for this effect an inclined orbit can be used [12]. Alternately, tracking the spacecraft near perihelion may allow the signature of the J_2 perturbation to be recognized and discriminated without having to resort to an inclined orbit.

One approach to disentangle the parameters β and γ in Eq. (2.29) would be to rely on experiments which determine γ separately [6,15]. However, as we show in the subsequent sections, β and γ can actually be disentangled in a single mission measuring the deflection of a spacecraft.

In order to extract the general relativistic contribution to the spacecraft's trajectory from a mission such as the Small Interstellar Probe it will be necessary to deal with perturbing non-gravitational forces. For a typical spacecraft these forces arise from radiation pressure, solar wind, interplanetary dust, atmospheric drag, magnetic fields, propellant leakage, and spacecraft radiation [4,16]. There are two ways to address these perturbations: They can be measured directly by placing sufficiently sensitive accelerometers on-board the spacecraft, and then treating these accelerometers as data which allow the non-gravitational forces to be directly estimated. However, it is likely that another technique will be necessary to sidestep these perturbations, which is to employ a drag-free spacecraft using small thrusters to null out the non-gravitational forces. Fortunately the necessary drag-free technology is already under development, since it is a prequisite for the ongoing Gravity Probe B mission [17], as well as for the proposed STEP [18] and Galileo Galilei [19] missions.

In the next section we develop the theoretical formalism needed to demonstrate how β and γ can be disentangled (at least in principle) in a single spacecraft deflection mission through an appropriate set of measurements. Using this formalism we show that a satellite deflection experiment may be able to separately determine β and γ to a precision of $\sim 4\times 10^{-5}$ and $\sim 8\times 10^{-6}$, respectively.

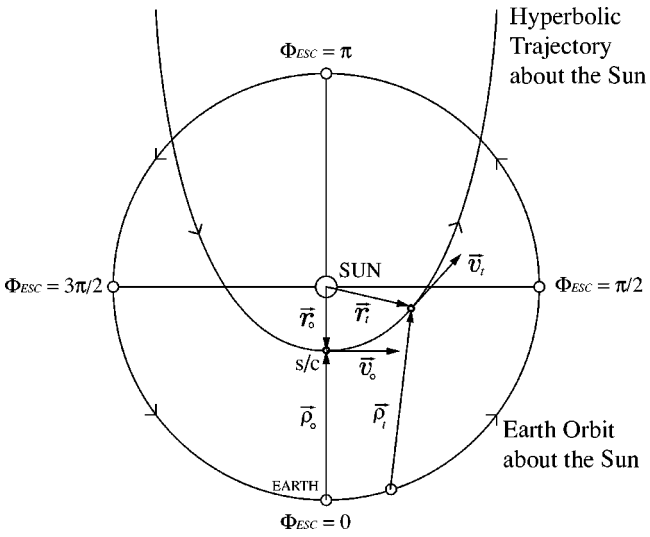

FIG. 3. Geometry of the spacecraft trajectory, where the spacecraft position and velocity vectors are $\vec{r}$ and $\vec{v}$. The Earth-to-spacecraft position vector is $\vec{\rho}$. Subscripts "o" and "t" refer to initial and later epochs. The location of the Earth with respect to the spacecraft at perihelion is indicated by the phase angle, Φ_{ESC}. Measurements of β and γ are computed assuming the optimal location of the Earth (Φ_{ESC}).

IV. ESTIMATING GENERAL RELATIVITY PARAMETERS FROM RADIOMETRIC TRACKING OF HELIOCENTRIC TRAJECTORIES

A. General

In this section we analyze in greater detail the precision to which we can determine the general relativistic parameters β and γ by measuring spacecraft trajectories. Specifically, we will focus on the question of disentangling β and γ by an appropriate set of measurements. In Sec. III an estimate of the necessary measurement accuracy of these parameters was made under a number of simplifying assumptions and approximations. In this section we relax some of these approximations and perform a more detailed and rigorous analysis of the problem. Figure 3 illustrates the geometry of the spacecraft trajectory. The spacecraft position and velocity vectors at perihelion are $\vec{r}_o$ and $\vec{v}_o$, and $\vec{\rho}_o$ is the Earth-to-spacecraft position vector at this time. The subscript "t" refers to these vectors at a later time. The phase angle at the initial time, Φ_{ESC}, is the Earth-Sun-Spacecraft angle. Figure 3 shows the Earth's location for $\Phi_{ESC}=0,\pi/2,\pi,$ and $3\pi/2$. (Since radiometric measurements are highly sensitive to the relative geometry of the spacecraft with respect to the Sun, we analyze estimates of β and γ as a function of Φ_{ESC}.) Although the analysis which follows is semi-analytical, it includes realistic models of the trajectory dynamics and measurement noise. We provide detailed estimates of how accurately the trajectory must be measured to set new limits on the parameters β and γ.

B. Transient effect of β and γ

From Ref. [2] (Sec. 7) the perturbing relativistic acceleration, to first PN order, can be written as (taking $G=c=1$ and noting that the spacecraft mass is much smaller than the solar mass)

$$\delta\vec{a}=\frac{m}{r^3}\left[2(\gamma+\beta)\frac{m\vec{r}}{r}-\gamma v^2\vec{r}+2(\gamma+1)(\vec{r}\cdot\vec{v})\vec{v}\right], \tag{4.1}$$

where $\vec{r}$ represents the spacecraft position vector and $\vec{v}$ represents the spacecraft velocity vector normalized by the speed of light. We note that the relativistic perturbation is present only in the orbital plane. The acceleration components decomposed into the radial (R), transverse (S), and out-of-plane (W) directions are

$$R=\frac{m^2(1+e\cos f)^2}{a^3(e^2-1)^3}[(1-e^2)\gamma+2\beta(1+e\cos f)+2(\gamma+1)e^2\sin^2 f], \tag{4.2a}$$

$$S=\frac{m^2(1+e\cos f)^2}{a^3(e^2-1)^3}[2(\gamma+1)(1+e\cos f)e\sin f], \tag{4.2b}$$

$$W=0. \tag{4.2c}$$

In Eqs. (4.2), a denotes the semi-major axis, e is the eccentricity of the orbit, and f is the true anomaly (to be distinguished from the mean anomaly M). The hyperbolic Lagrange planetary equations [20,21], with proper changes (i.e., $e^2>1$, $a\rightarrow -a$) can be represented as

$$\frac{da}{dt}=-\frac{2a^{3/2}}{\sqrt{m(e^2-1)}}[\mathrm{Re}\sin f+S(1+e\cos f)], \tag{4.3a}$$

$$\frac{de}{dt}=\sqrt{\frac{a(e^2-1)}{m}}\left[R\sin f+\frac{S}{e}\left(\frac{p}{r}+\frac{r}{a}\right)\right], \tag{4.3b}$$

$$\frac{di}{dt}=\frac{r}{h}W\cos(\omega+f), \tag{4.3c}$$

$$\frac{d\Omega}{dt}=\frac{rW\sin(\omega+f)}{h\sin i}, \tag{4.3d}$$

$$\frac{d\omega}{dt}=\frac{1}{e}\sqrt{\frac{a(e^2-1)}{m}}\left[-R\cos f+S\frac{2+e\cos f}{1+e\cos f}\sin f\right]-\frac{d\Omega}{dt}\cos i, \tag{4.3e}$$

$$\frac{dM}{dt}=n-\frac{1}{na}\left[\frac{2r}{a}-\frac{(e^2-1)}{e}\cos f\right]R+\frac{(e^2-1)}{nae}\left[\frac{r}{p}\right]S. \tag{4.3f}$$

In Eqs. (4.3) i is the orbit inclination, ω is the argument of periapsis, Ω is the longitude of the ascending node, and $n=\sqrt{m/|a|^3}$ is the normalized mean motion.

After substitution of the perturbing relativistic acceleration components from Eq. (4.2) into the hyperbolic Lagrange equations, the changes in the orbital elements from periapsis passage to some value of the true anomaly can be approximated by keeping the elements on the right-hand side constant and allowing the true anomaly to vary. We thus find

$$\Delta a=\frac{2em}{(e^2-1)^2}[(2+2\beta+3\gamma+2e^2+\gamma e^2)\Delta\cos f-(2+\beta+2\gamma)e\Delta\sin^2 f], \tag{4.4a}$$

$$\Delta e=-\frac{m}{a(e^2-1)}[(\gamma+2\beta+4e^2+3\gamma e^2)\Delta\cos f-(2+\beta+2\gamma)e\Delta\sin^2 f], \tag{4.4b}$$

$$\Delta\omega=\frac{m}{a(e^2-1)}\left[(2-\beta+2\gamma)\Delta f-\left(\frac{2\beta+(1-e^2)\gamma}{e}\right)\Delta\sin f-(2+\beta+2\gamma)\Delta(\sin f\cos f)\right], \tag{4.4c}$$

$$\Delta M=\frac{3m}{a(e^2-1)^2}[\gamma+\beta+(2+\gamma)e^2+(2+3\gamma+2\beta+(2+\gamma)e^2)e+(2+2\gamma+\beta)e^2]n\Delta t-\frac{m}{a\sqrt{e^2-1}}\left[(2+2\gamma+\beta)\Delta(\sin f\cos f)+\frac{\gamma+2\beta+(4+3\gamma)e^2}{e}\Delta\sin f\right]-(2+\gamma)\frac{m}{a}\Delta F, \tag{4.4d}$$

where F is the hyperbolic eccentric anomaly [note that Δt in Eq. (4.4d) is the actual time multiplied by the speed of light c].

Figures 4 and 5 show the change in the orbital elements due to the relativistic effect. The initial epoch is at the periapsis with $r_p=4r_\odot$ and $V_\infty=39$ km/s, where r_p and $r_\odot$ are the perihelion distance and radius of the Sun, respectively. A conclusion that we draw by studying these perturbations is that most of the changes in orbital elements due to GR occur very early in the trajectory (usually within a few days of perihelion).

Of most interest are the partial derivatives of the orbital elements with respect to the relativistic constants, β and γ, based on Eqs. (4.4). These indicate the sensitivity of the trajectory to the PPN parameters, and give us an indication of the information content related to β and γ in the trajec-

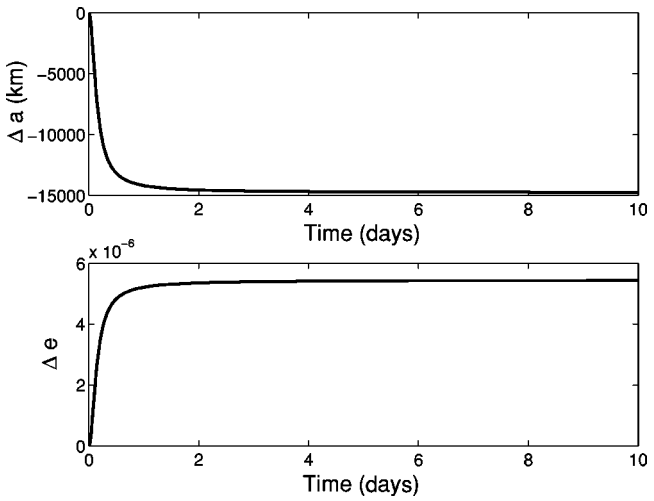

FIG. 4. Change in the semi-major axis Δa and eccentricity Δe due to the relativistic effect. These figures, as well as Fig. 5(a), indicate that most of the GR effects are observable within a few days of perihelion.

tory. If we let E be the set of orbital elements, a change in E due to relativistic effects can be represented as $E=E_o+\Delta E$, where E_o denotes the initial orbital elements. Taking partials with respect to the GR parameters yields

$$\frac{\partial E}{\partial(\gamma,\beta)}=\frac{\partial(E_o+\Delta E)}{\partial(\gamma,\beta)}=\frac{\partial\Delta E}{\partial(\gamma,\beta)}. \tag{4.5}$$

We will use these partials later to form the state transformation from the GR parameters to the data measurements. The partial derivatives of the orbital elements with respect to γ are given by

$$\frac{\partial a}{\partial\gamma}=-\frac{2em}{(e^2-1)^2}[(3+e^2)(1-\cos f)+2e\sin^2 f], \tag{4.6a}$$

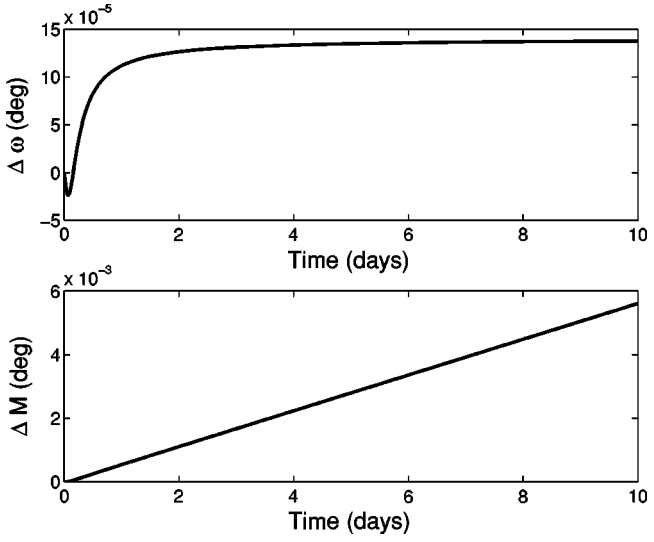

FIG. 5. Change in the argument of perihelion $\Delta\omega$, and mean anomaly ΔM, due to the relativistic effect. See also caption to Fig. 4.

$$\frac{\partial e}{\partial\gamma}=\frac{m}{a(e^2-1)}[(1+3e^2)(1-\cos f)+2e\sin^2 f], \tag{4.6b}$$

$$\frac{\partial\omega}{\partial\gamma}=\frac{m}{a(e^2-1)}\left[2f-2\sin f\cos f+\frac{(e^2-1)}{e}\sin f\right], \tag{4.6c}$$

$$\frac{\partial M}{\partial\gamma}=\frac{3m}{a(e^2-1)^2}[1+3e+3e^2+e^3]M-\frac{m}{a\sqrt{e^2-1}}\left[2\sin f\cos f+\frac{(1+3e^2)}{e}\sin f\right]-\frac{m}{a}F. \tag{4.6d}$$

Similarly, the partial derivatives of the orbital elements with respect to β are

$$\frac{\partial a}{\partial\beta}=-\frac{2em}{(e^2-1)^2}[2(1-\cos f)+e\sin^2 f], \tag{4.7a}$$

$$\frac{\partial e}{\partial\beta}=\frac{m}{a(e^2-1)}[2(1-\cos f)+e\sin^2 f], \tag{4.7b}$$

$$\frac{\partial\omega}{\partial\beta}=\frac{m}{a(e^2-1)}\left[-f-\frac{2\sin f}{e}-\sin f\cos f\right], \tag{4.7c}$$

$$\frac{\partial M}{\partial\beta}=\frac{3m}{a(e^2-1)^2}[1+2e+e^2]M-\frac{m}{a\sqrt{e^2-1}}\left[\sin f\cos f+\frac{2}{e}\sin f\right]. \tag{4.7d}$$

Figures 6–8 show how the partial derivatives of the orbital elements with respect to the GR parameters change as the spacecraft travels on the hyperbolic trajectory, where the initial conditions are the same as assumed above. It is crucial to note that the partials of ω with respect to β and γ are quite different from each other—not only their signs, but also their ratios. These partials essentially represent the amount of information contained in our measurements of β and γ, and thus their ratios represent the correlation between β and γ. The slow convergence of the ratio of the partials with respect to ω in Fig. 8, as compared to the other ratios, shows that there is a possibility of obtaining *separate* estimates of the PPN parameters by tracking the spacecraft close to perihelion, which is a novel feature of the GR test we are proposing.

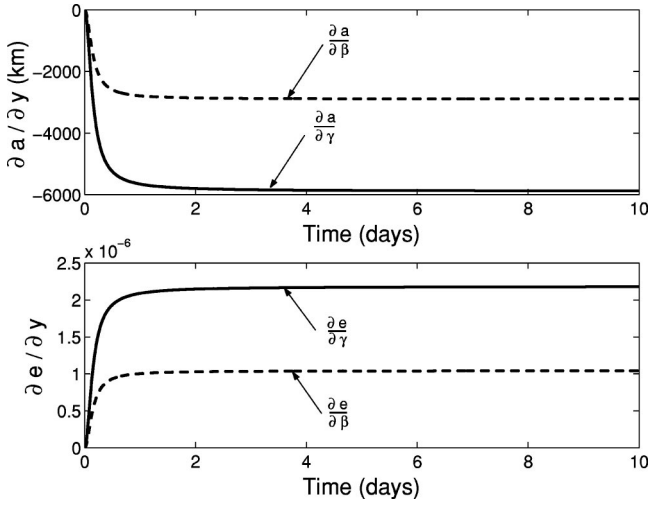

FIG. 6. Change in the partial derivatives of semi-major axis and eccentricity with respect to the GR parameters. The variable y denotes either β or γ as appropriate.

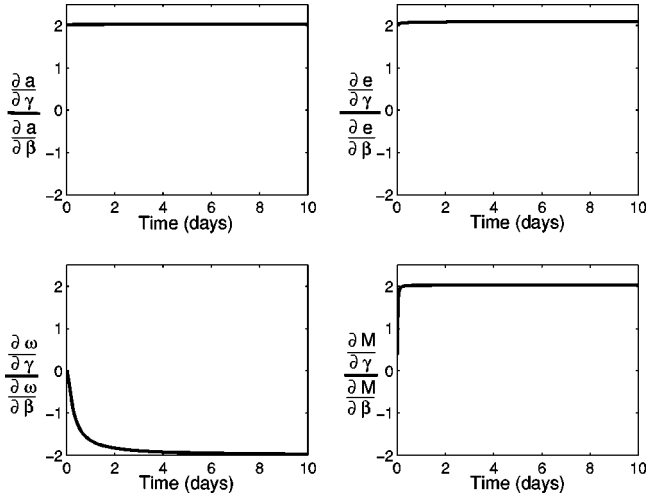

FIG. 8. Ratios of orbital-element partial derivatives with respect to the GR parameters. The time variation for ω (lower left plot) demonstrates the potential to separately determine β and γ.

V. COVARIANCE ANALYSIS AND LEAST SQUARES APPROXIMATION

A. Measurement data types

Having established the sensitivity of the trajectory to β and γ, we can consider estimates of how well β and γ can be determined by measuring the trajectory (Fig. 3). For our analysis, three different measurement data types are considered. The first is a two-way radar range measurement (Z_ρ), which measures the distance between the spacecraft and the tracking station based on the travel time of the uplink and downlink signals. The second data type we consider is VLBI measurements ($Z_{m,n}$), which measure the longitudinal and latitudinal angles of the spacecraft trajectory in the plane of the sky at the location of the tracking station [22]. Combined with range measurements, VLBI can determine the 3-dimensional position of the spacecraft. The final data type we consider is Doppler measurements, $Z_{\dot\rho}$, which measure the frequency shift (Doppler effect) in the transmitted signals. The frequency shift directly gives the range rate and, due to the Hamilton-Melbourne effect [23], provides angular information on the trajectory. All of these measurement data types are analyzed using a variety of phase angles between the Earth and the spacecraft trajectory—i.e., the initial Earth-Sun-spacecraft angle, Φ_{ESC}, as shown in Fig. 3.

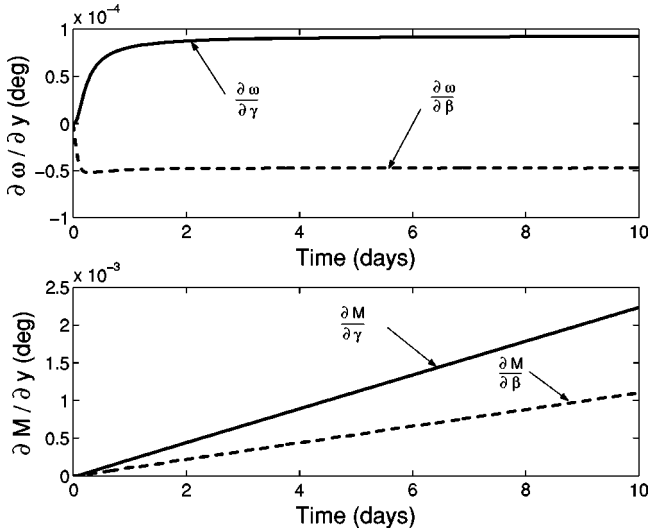

FIG. 7. Change in the partial derivatives of the argument of perihelion and mean anomaly with respect to the GR parameters. The variable y denotes β or γ as appropriate.

B. State to be estimated

At epoch, the spacecraft is located at perihelion of its heliocentric trajectory with the orbital elements

$$a_o = 8.725\times 10^7 \ \text{(km)},$$

$$e_o = 1.0319,$$

$$i_o = \omega_o = \Omega_o = M_o = 0. \tag{5.1}$$

These elements, in addition to the PPN parameters β and γ, define the epoch state of our system: $Y_o = [\vec{r}_o\ \vec{v}_o\ \gamma\ \beta]^T = [x_o\ y_o\ z_o\ u_o\ \nu_o\ w_o\ \gamma\ \beta]^T$. The trajectories of the spacecraft and of the Earth are assumed to be coplanar. (We are ignoring the issue of disentangling the effect of J_2 in this analysis.) The spacecraft escapes the Sun with $V_\infty = 39$ km/s, which corresponds to a periapsis velocity of $V_p = 311$ km/s.

The hypothetical trajectory from Ref. [1] will most likely fly into perihelion as an elliptic orbit and then boost to a hyperbolic escape trajectory. Hence the initial state, Eqs. (5.1), can be considered as the condition at epoch. Table II presents the conservative initial uncertainties that are assumed at epoch for the initial covariance matrix (assuming an accurate on-board measurement of the ΔV maneuver applied at perihelion).

TABLE II. Assumed initial uncertainties for various physical quantities.

Quantity	$\sigma_{xx},\sigma_{yy},\sigma_{zz}$ (km^2)	$\sigma_{uu},\sigma_{\nu\nu},\sigma_{ww}$ (km^2/s^2)	$\sigma_{\beta\beta},\sigma_{\gamma\gamma}$	σ_{ij} for $i\neq j$
Uncertainty	1	10^{-6}	1	0

C. Computation of the information and covariance matrix

To compute the state uncertainty at epoch, given a number of measurements, requires the computation of the information matrix Λ, which is given by

$$\Lambda=\left[\sum_i^N \frac{1}{\sigma_i^2}\left(\frac{\partial Z_i(Y_o)}{\partial Y_o}\right)_o^T\left(\frac{\partial Z_i(Y_o)}{\partial Y_o}\right)_o\right]. \tag{5.2}$$

Here Z_i are the measurements, σ_i are the noise factors in the measurements, Y_o is the epoch state, and N is the number of measurements taken. Given the information matrix, the covariance matrix P of the initial state and the GR parameters is then

$$P=\Lambda^{-1}, \tag{5.3}$$

where $P_{ij}=\sigma_{ij}$ for $i,j\in\{x_o,y_o,z_o,u_o,\nu_o,w_o,\gamma,\beta\}$. The standard deviation in our measured γ or β parameter will then be $\sigma_\gamma=\sqrt{\sigma_{77}}$ and $\sigma_\beta=\sqrt{\sigma_{88}}$ and their correlation will be $\sigma_{78}/\sigma_\gamma\sigma_\beta$.

The initial uncertainties in Eq. (5.3) are provided by Table II. It follows from Eq. (5.2) that to compute the information matrix we must analyze the sensitivity of a measurement with respect to the initial conditions and the GR parameters:

$$\frac{\partial Z}{\partial Y_o}=\left(\frac{\partial Z}{\partial X}\right)\left(\frac{\partial X}{\partial E}\right)\left(\frac{\partial E}{\partial W_o}\right)\left(\frac{\partial W_o}{\partial Y_o}\right), \tag{5.4}$$

where

$$W_o=[a_o\ \ e_o\ \ i_o\ \ \omega_o\ \ \Omega_o\ \ M_o\ \ \gamma_o\ \ \beta_o]^T, \tag{5.5a}$$

$$E=[a\ \ e\ \ i\ \ \omega\ \ \Omega\ \ M]^T, \tag{5.5b}$$

$$X=\begin{bmatrix}\vec{r}\\ \vec{v}\end{bmatrix}=\begin{bmatrix}\tilde{x}\mathbf{P}+\tilde{y}\mathbf{Q}\\ \dot{\tilde{x}}\mathbf{P}+\dot{\tilde{y}}\mathbf{Q}\end{bmatrix}=[x\ \ y\ \ z\ \ u\ \ \nu\ \ w]^T. \tag{5.5c}$$

For the current analysis these partials are computed analytically, and the initial values of the variables are denoted by the subscript "o." (Figure 3 depicts $\vec{\rho}_o$, $\vec{r}_o$, and $\vec{v}_o$.)

The Gaussian vectors **P** and **Q** are functions of the orbital elements i,ω, and Ω and define the geometry of the orbit in space (Ref. [20], Sec. 2.7). The scalars $\tilde{x}$ and $\tilde{y}$ are functions of the orbital elements a, e, and M which define the coordinates inside the orbital plane. The Gaussian vectors **P** and **Q** are constant and can be computed based on the initial epoch, whereas $\tilde{x}$ and $\tilde{y}$ must be computed at each instant in time. Finally, Z denotes the data measurement.

D. Implementation of the analysis

We can exhibit the partial derivatives of the initial orbital elements and the GR parameters with respect to the initial position, velocity, and the GR parameters as an 8×8 matrix, represented as follows:

$$\frac{\partial W_o}{\partial Y_o}=\begin{bmatrix}\left(\frac{\partial E(t_o)}{\partial X(t_o)}\right)_{6\times6} & 0_{6\times2}\\ 0_{2\times6} & I_{2\times2}\end{bmatrix}. \tag{5.6}$$

Here, $\partial E(t_o)/\partial X(t_o)$ is the inverse of $\partial X(t_o)/\partial E(t_o)$ and can be obtained from the analytic relations

$$\left(\frac{\partial E(t_o)}{\partial X(t_o)}\right)=\left(\frac{\partial X(t_o)}{\partial E(t_o)}\right)^{-1}=P(E,E)\left[\left(+\frac{\partial\vec{v}(t_o)}{\partial E(t_o)}\right)^T\left(-\frac{\partial\vec{r}(t_o)}{\partial E(t_o)}\right)^T\right], \tag{5.7}$$

where P is an antisymmetric 6×6 matrix made up of the Poisson brackets

$$P(E_i,E_j)=\left(\frac{\partial E_i}{\partial\vec{r}}\right)\left(\frac{\partial E_j}{\partial\vec{v}}\right)^T-\left(\frac{\partial E_j}{\partial\vec{r}}\right)\left(\frac{\partial E_i}{\partial\vec{v}}\right)^T. \tag{5.8}$$

Although the computation of P is quite complicated, there exist only five independent nonzero terms [20]:

$$P(a,M)=-P(M,a)=+\frac{2}{na}, \tag{5.9a}$$

$$P(e,\omega)=-P(\omega,e)=\frac{\sqrt{e^2-1}}{na^2e}, \tag{5.9b}$$

$$P(e,M)=-P(M,e)=\frac{e^2-1}{na^2e}, \tag{5.9c}$$

$$P(i,\Omega)=-P(\Omega,i)=+\frac{1}{na^2\sqrt{e^2-1}\sin i}, \tag{5.9d}$$

$$P(i,\omega)=-P(\omega,i)=\frac{1}{na^2\sqrt{e^2-1}\tan i}. \tag{5.9e}$$

It is important to note that these partials can be calculated based on the initial conditions, and are constants throughout the numerical computation.

We next consider the partial derivatives of the orbital elements with respect to the initial orbital elements and the GR parameters. These can be considered as the orbital-element transition matrix plus the partial derivatives of the orbital elements with respect to the GR parameters given in Sec. IV. For an unperturbed hyperbolic Keplerian orbit, the orbital elements are constants except for the mean anomaly $M(t)$, which can be represented as

$$M(t)-M(t_o)=n(t-t_o). \tag{5.10}$$

The partial derivatives of the orbital elements with respect to the initial orbital elements and the GR parameters can be written as

$$\frac{\partial E}{\partial W_o}=\left[\left(\frac{\partial E(t)}{\partial E(t_o)}\right)_{6\times 6}\left(\frac{\partial E(t)}{\partial(\gamma,\beta)}\right)_{6\times 2}\right]. \tag{5.11}$$

The mean motion is a function of the semi-major axis, a, and hence the orbital-element transition matrix, $\partial E(t)/\partial E(t_o)$, gives rise to a 6×6 identity matrix with one non-vanishing off-diagonal element:

$$\frac{\partial M(t)}{\partial a(t_o)}=-\frac{3n}{2a}(t-t_o). \tag{5.12}$$

The partial derivatives of the orbital elements with respect to the GR parameters are given in Eqs. (4.6) and (4.7).

Next we consider the partial derivatives $(\partial X/\partial E)$ of the state vector with respect to the orbital elements, which can be represented by a 6×6 matrix:

$$\frac{\partial X}{\partial E}=\begin{bmatrix} \frac{\partial\tilde{x}}{\partial a}\mathbf{P}+\frac{\partial\tilde{y}}{\partial a}\mathbf{Q} & \frac{\partial\tilde{x}}{\partial e}\mathbf{P}+\frac{\partial\tilde{y}}{\partial e}\mathbf{Q} & \tilde{x}\frac{\partial\mathbf{P}}{\partial i}+\tilde{y}\frac{\partial\mathbf{Q}}{\partial i} & \tilde{x}\frac{\partial\mathbf{P}}{\partial\omega}+\tilde{y}\frac{\partial\mathbf{Q}}{\partial\omega} & \tilde{x}\frac{\partial\mathbf{P}}{\partial\Omega}+\tilde{y}\frac{\partial\mathbf{Q}}{\partial\Omega} & \frac{\partial\tilde{x}}{\partial M}\mathbf{P}+\frac{\partial\tilde{y}}{\partial M}\mathbf{Q} \\ \frac{\partial\dot{\tilde{x}}}{\partial a}\mathbf{P}+\frac{\partial\dot{\tilde{y}}}{\partial a}\mathbf{Q} & \frac{\partial\dot{\tilde{x}}}{\partial e}\mathbf{P}+\frac{\partial\dot{\tilde{y}}}{\partial e}\mathbf{Q} & \dot{\tilde{x}}\frac{\partial\mathbf{P}}{\partial i}+\dot{\tilde{y}}\frac{\partial\mathbf{Q}}{\partial i} & \dot{\tilde{x}}\frac{\partial\mathbf{P}}{\partial\omega}+\dot{\tilde{y}}\frac{\partial\mathbf{Q}}{\partial\omega} & \dot{\tilde{x}}\frac{\partial\mathbf{P}}{\partial\Omega}+\dot{\tilde{y}}\frac{\partial\mathbf{Q}}{\partial\Omega} & \frac{\partial\dot{\tilde{x}}}{\partial M}\mathbf{P}+\frac{\partial\dot{\tilde{y}}}{\partial M}\mathbf{Q} \end{bmatrix}_{6\times 6}. \tag{5.13}$$

For a given initial condition, we can compute each of these partials based on two-body relations [20,24]. With proper changes (i.e. $a\rightarrow -a$), the equations for two-body hyperbolic motions yield the relations

$$r=a(e\cosh F-1),\quad \tilde{x}=a(e-\cosh F),\quad \dot{\tilde{x}}=\frac{\sqrt{ma}}{r}\sinh F,\quad \tilde{y}=a\sqrt{e^2-1}\sinh F,\quad \dot{\tilde{y}}=\frac{\sqrt{ma}}{r}\sqrt{e^2-1}\cosh F, \tag{5.14}$$

where we solve for the hyperbolic eccentric anomaly (F) using the modified Kepler's equation [21]

$$\sqrt{\frac{m}{|a|^3}}(t-\tau)=e\sinh(F)-F, \tag{5.15}$$

where τ is the time of perihelion passage. We now take the partials of the coordinates $\tilde{x}$ and $\tilde{y}$ and their time derivatives, $\dot{\tilde{x}}$ and $\dot{\tilde{y}}$, with respect to the orbital elements a, e, and M, which gives

$$\frac{\partial(\tilde{x},\tilde{y})^T}{\partial(a,e,M)^T}=\begin{bmatrix} \frac{\tilde{x}}{a} & \left(a+\frac{\tilde{y}^2}{r(e^2-1)}\right) & \frac{\dot{\tilde{x}}}{n} \\ \frac{\tilde{y}}{a} & -\left(\frac{\tilde{x}\tilde{y}}{r(e^2-1)}\right) & \frac{\dot{\tilde{y}}}{n} \end{bmatrix}, \tag{5.16}$$

$$\frac{\partial(\dot{\tilde{x}},\dot{\tilde{y}})^T}{\partial(a,e,M)^T}=\begin{bmatrix} -\frac{\dot{\tilde{x}}}{2a} & -\dot{\tilde{x}}\left(\frac{a}{r}\right)^2\left(2\left(\frac{\tilde{x}}{a}\right)+\frac{e}{e^2-1}\left(\frac{\tilde{y}}{a}\right)^2\right) & -n\left(\frac{a}{r}\right)^3\tilde{x} \\ -\frac{\dot{\tilde{y}}}{2a} & -\frac{n}{\sqrt{e^2-1}}\left(\frac{a}{r}\right)^2\left(\frac{\tilde{x}^2}{r}-\frac{\tilde{y}^2}{a(e^2-1)}\right) & -n\left(\frac{a}{r}\right)^3\tilde{y} \end{bmatrix}. \tag{5.17}$$

The partials of **P** and **Q** with respect to i, ω, and Ω are provided in Ref. [20] (Sec. 7). We note that these partials are constants with respect to time, and can be evaluated based on the spacecraft's initial epoch.

Next we evaluate the partial derivatives $\partial Z/\partial X$ of the data measurements with respect to the state vector. The first data type we consider are range measurements

$$Z_\rho = |\vec{r} - \vec{r}_E - \vec{r}_{TS}| = |\vec{\rho}|, \tag{5.18}$$

the distance between the spacecraft and the tracking station (TS). The vector $\vec{r}_E$ represents the position of the Earth (with respect to the Sun) whose orbit is assumed to be circular with 1 year period and radius of 1 AU. The partial derivative of Z_ρ with respect to X is given by

$$\frac{\partial Z_\rho}{\partial X} = = \begin{bmatrix} \hat{\rho}(t) \\ 0_{3\times 1} \end{bmatrix}^T_{6\times 1}, \tag{5.19}$$

where $\hat{\rho}$ is the unit position vector of the spacecraft as measured from the Earth (Fig. 3). We consider several assumed values for the precision of the range measurement, σ_ρ, in the interval 10^{-4} km$\leqslant \sigma_\rho \leqslant 10^{-2}$ km.

An additional measurement data type considered is VLBI, which yields accurate angular measurements of the spacecraft relative to a radio source. We represent this measurement as a set of angles,

$$Z_{(m,n)} = \begin{bmatrix} Z_m & Z_n \end{bmatrix}^T, \tag{5.20}$$

where Z_m and Z_n are the longitudinal and the latitudinal angular measurements, respectively. Taking partials with respect to X yields

$$\frac{\partial Z_{(m,n)}}{\partial X} = \begin{bmatrix} \dfrac{\hat{m}_o^T}{\rho} & 0_{1\times 3} \\ \dfrac{\hat{n}_o^T}{\rho} & 0_{1\times 3} \end{bmatrix}_{2\times 6}, \tag{5.21}$$

where we define

$$\hat{l}_o = \hat{\rho},$$

$$\hat{m}_o = \hat{l}_o \times \hat{n}_o,$$

$$\hat{n}_o = \frac{\hat{z} - (\hat{z}\cdot\hat{l}_o)\hat{l}_o}{|\hat{z} - (\hat{z}\cdot\hat{l}_o)\hat{l}_o|}, \tag{5.22}$$

where $\hat{z} = [0\ 0\ 1\ ]^T$. In Eq. (5.21) ρ is the range from Earth to the spacecraft as defined earlier. The precisions assumed for the angular measurements are 5, 1, and 0.1 nrad.

The final data measurement type we analyze is Doppler,

$$Z_{\dot\rho} = \frac{d}{dt}|\vec{r} - \vec{r}_E - \vec{r}_{TS}| = \hat{\rho}\cdot\dot{\vec{\rho}}, \tag{5.23}$$

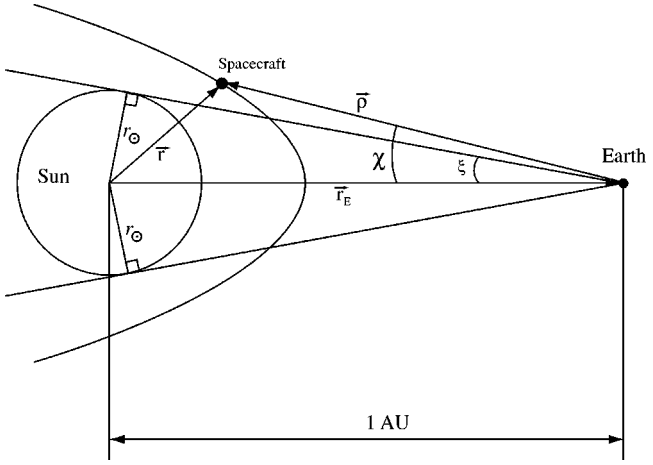

FIG. 9. Occulation effect due to the Sun. No radiometric measurements can be made when the spacecraft passes in front of (or behind) the Sun. See text for further details.

which is widely used for interplanetary missions. These measurements determine the shift in frequency due to the Doppler effect, and contain both range and angular information. The partial derivative of $Z_{\dot\rho}$ results in

$$\frac{\partial Z_{\dot\rho}}{\partial X} = \begin{bmatrix} \dfrac{\partial \hat{\rho}}{\partial \vec{r}}\cdot\dot{\vec{\rho}} \\ \hat{\rho} \end{bmatrix}^T_{6\times 1}, \tag{5.24}$$

where

$$\frac{\partial \hat{\rho}}{\partial \vec{r}} = \frac{1}{\rho}[I_3 - \hat{\rho}\hat{\rho}^T], \tag{5.25}$$

and I_3 is the unit 3×3 matrix. The accuracies, $\sigma_{\dot\rho}$, assumed for the Doppler measurement are 10^{-6}, 10^{-7}, and 10^{-8} km/s for integration over a 60-s period.

E. Solar occultation effects

When the spacecraft passes in front of (or behind) the Sun (Fig. 9), radiometric measurements cannot be obtained. Since the trajectory originates close to the Sun, solar interference of the measurements can be an important effect in the early stage of the experiment. Let us define

$$\chi = \cos^{-1}\left[\frac{\vec{\rho}\cdot(-\vec{r}_E)}{\rho r}\right], \tag{5.26}$$

where χ represents the spacecraft-Earth-Sun angle. Based on the geometry of the Earth and Sun, and assuming that the Earth is in circular orbit about the Sun, the angle between $\vec{r}_E$ and the tangent vector from center of the Earth to the outer radius of the Sun, ξ, can be computed and its value is approximately 0.267°. We assume that no Doppler or VLBI measurements are taken if $\chi \leqslant \xi + 0.5°$, corresponding to approximately $3r_\odot$, and that no range measurements are taken if $\chi \leqslant \xi + 5°$, corresponding to approximately $20r_\odot$. The effects of measurement geometry and solar occulations on the

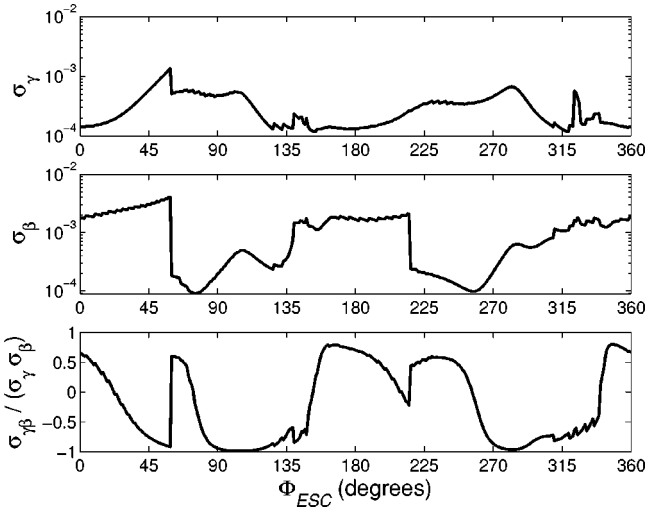

FIG. 10. Dependence of measurement accuracies and correlations of β and γ on the phase angle, Φ_{ESC}, of the Earth.

accuracies and correlations of β and γ depend on the phase angle of the Earth, Φ_{ESC}, as shown in Fig. 10.

VI. RESULTS

For our analysis, the spacecraft is assumed to be initially at periapsis of the heliocentric hyperbolic trajectory, with $r_p = 4r_\odot$ and $V_\infty = 39$ km/s. All of the data measurements considered are analyzed with different initial phase angles (Φ_{ESC}) in order to study the sensitivity of β and γ estimates to Φ_{ESC} (Fig. 10). The measurements are assumed to be taken every 15 min over a 10-day time span. It is important to note that uncertainties in β and γ vary over an order of magnitude, which indicates that the relative geometry of the spacecraft with respect to the tracking station is a critical factor in this test. The results of this analytical approach are consistent with numerical simulations that were carried out.

The results shown in Figs. 11 and 12 are based on tracking the spacecraft under the same data schedule as defined above, except that we disregard the solar occultation effect (which provides a lower bound on the uncertainty in our β and γ estimates). Figure 11 shows the uncertainties in β and γ when the range, VLBI, and Doppler measurements are combined. The plots of σ_γ and σ_β are shown for "standard accuracy" and "advanced accuracy" which we characterize as follows. Standard technology can provide noise factors of $\sigma_\rho = 10^{-3}$ km, $\sigma_{\dot\rho} = 10^{-7}$ km/s, and $\sigma_{\angle\rho} = 1$ nrad using *X*-band radiometric tracking. These noise factors are directly related to how much information can be obtained from the spacecraft trajectory. Advanced accuracy noise factors are one order of magnitude more sensitive than the standard accuracy case, and are consistent with the *K*-band radiometric tracking system.

Figure 12 shows the correlations between σ_γ and σ_β (i.e., $\sigma_{78}/\sigma_\gamma\sigma_\beta$). We observe that the GR parameters become more correlated as the spacecraft moves away from periapsis. Thus, as time increases, the most accurate determinations of the PPN parameters may be correlated with each other, but

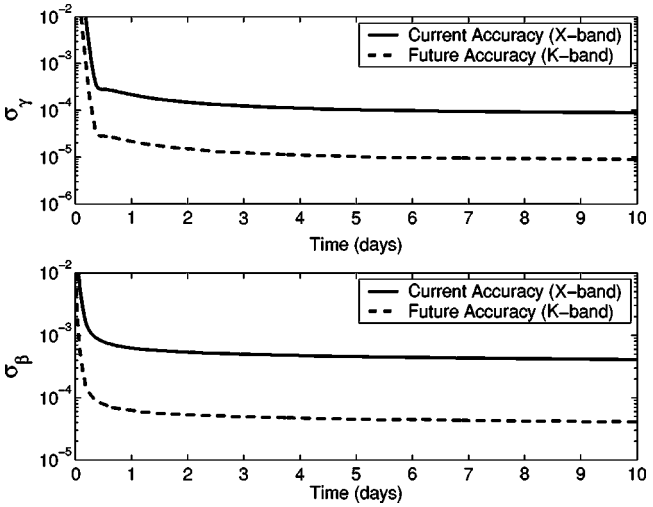

FIG. 11. Uncertainties in β and γ determinations as functions of time for standard and advanced tracking accuracies. Standard accuracy (*X* band) assumes $\sigma_\rho = 10^{-3}$ km, $\sigma_{\dot\rho} = 10^{-7}$ km/s, and $\sigma_{\angle\rho} = 1$ nrad for range, range rate, and cross track uncertainties, respectively. Advanced accuracy (*K* band) assumes $\sigma_\rho = 10^{-4}$ km, $\sigma_{\dot\rho} = 10^{-8}$ km/s, and $\sigma_{\angle\rho} = 0.1$ nrad. In the legend "current" refers to standard technology, and "future" refers to advanced technology.

determinations made using fewer data (and hence with reduced precision) may be less correlated. This is a subtle issue and should be investigated in more detail to determine how the measurement of β may be optimized with respect to γ.

Our results are summarized in Table III. All of the values of σ_β and σ_γ shown in Table III are the final ones taken at the end of the time span, without the solar occultation effect, thus indicating how accurately the GR parameters can be determined. Two obvious ways to increase the accuracy of these parameters are to either take more measurements or to improve the noise factors. It is important to note, however, that our analysis neglects a number of possible systematic error sources that may be present in the measurements.

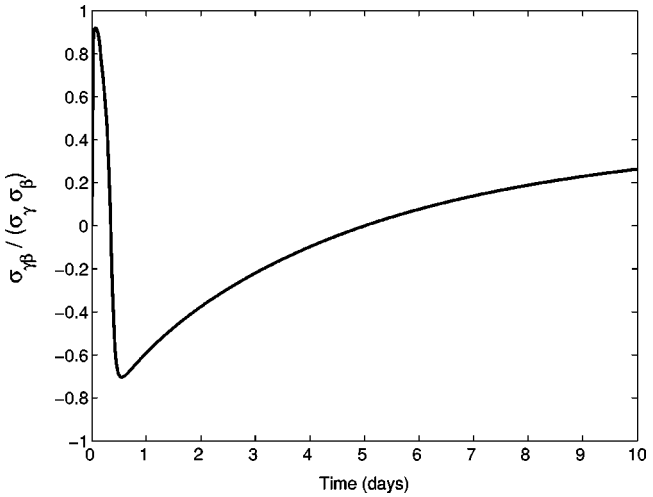

FIG. 12. Correlation of β and γ for range, VLBI, and Doppler measurements, with standard accuracies $\sigma_\rho = 10^{-3}$ km, $\sigma_{\dot\rho} = 10^{-7}$ km/s, and $\sigma_{\angle\rho} = 1$ nrad.

TABLE III. Uncertainties σ_β and σ_γ in the determination of the PPN parameters β and γ, respectively, for various assumed uncertainties in range, VLBI, and Doppler measurements, as described in the text. The time span for the measurements is 30 days.

Accuracy status	σ_ρ (km)	$\sigma_{\dot\rho}$ (km/s)	$\sigma_{\angle\rho}$ (nrad)	σ_β	σ_γ
Standard (X band)	10^{-3}	10^{-7}	1	3.7×10^{-4}	7.8×10^{-5}
Advanced (K band)	10^{-4}	10^{-8}	0.1	3.7×10^{-5}	7.8×10^{-6}

Based on these results, we find that the original discussion in Ref. [1] is conservative, and that tracking technology currently being implemented may already allow this experiment to determine the PPN parameters β and γ to an accuracy of $\sim4\times10^{-4}$ and $\sim8\times10^{-5}$, respectively (as shown in Table III). By performing a detailed covariance analysis of the proposed experiment, the full strength of the range and Doppler radiometric data can be accounted for, weakening the requirement for highly accurate VLBI measurements. There are, however, additional issues that must still be addressed. The current results serve as an impetus to continue this investigation, as we have determined that the spacecraft trajectory clearly has sufficient information content to allow for this unique measurement to be performed. Work in progress will include the effects of solar oblateness, solar radiation pressure, and systematic measurement errors in an analysis of this experiment.

Note added. After this work was completed, we learned of similar research by Vulkov [25].

ACKNOWLEDGMENTS

We are indebted to Jennifer Coy, Damon Landau, Anastassios Petropoulos, Nancy M. Schnepp, and Sharon Wise for their assistance in preparing this paper. The work of E.F. was supported in part by the U.S. Department of Energy under Contract No. DE-AC02-76ER01428. D.J.S. acknowledges support from the IND Technology Program by a grant from the Jet Propulsion Laboratory, California Institute of Technology, which is under contract with the National Aeronautics and Space Administration.

[1] J.M. Longuski, E. Fischbach, and D.J. Scheeres, Phys. Rev. Lett. **86**, 2942 (2001).
[2] C.M. Will, *Theory and Experiment in Gravitational Physics*, revised ed. (Cambridge University Press, Cambridge, England, 1993).
[3] H.C. Ohanian and R. Ruffini, *Gravitation and Spacetime* (Norton, New York, 1994).
[4] I. Ciufolini and J.A. Wheeler, *Gravitation and Inertia* (Princeton University Press, Princeton, 1995), pp. 339, 495.
[5] E. Fischbach and C. Talmadge, *The Search for Non-Newtonian Gravity* (AIP/Springer-Verlag, New York, 1999).
[6] B. Bertotti, L. Iess, and P. Tortora, Nature (London) **425**, 374 (2003).
[7] S. Weinberg, *Gravitation and Cosmology: Principles and Applications of the General Theory of Relativity* (Wiley & Sons, New York, 1972).
[8] *Handbook of Chemistry and Physics*, 65th ed., edited by R.C. Weast (CRC Press, Boca Raton, 1984).
[9] A.V. Labunsky, O.V. Papkov, and K.G. Sukhanov, *Multiple Gravity Assist Interplanetary Trajectories*, 1st ed. (Gordon and Breach, Amsterdam, 1998), p. 14.
[10] R.A. Mewaldt, J. Kangas, S.J. Kerridge, and M. Neugebauer, Acta Astron. **35**, 267 (1995); Data Systems, CCSDS B20.0-Y-1, Yellow Book, 1994.
[11] J.S. Border and J.A. Koukos, in Proceedings of the RF and Modulation Subpanel 1E Meeting, edited by T.M. Nguyen, Consultative Committee for Space Data Systems, CCSDS B20.0-Y-1, Yellow Book, 1994, Accademia Nazionale dei Lincei, Rome, 1977, pp. 393–442.
[12] K.D. Mease, J.D. Anderson, L.J. Wood, and L.K. White, J. Guid. Control Dyn. **7**, 36 (1984); J.D. Anderson, G. Colombo, L.D. Friedman, and E.L. Lau, in *Gravitazione Sperimentale* (Accademia Nazionale dei Lincei, Rome, 1977), pp. 393–442.
[13] R.N. Treuhaft and S.T. Lowe, Astron. J. **102**, 1879 (1991).
[14] R.N. Treuhaft and S.T. Lowe, Jet Propulsion Laboratory TDA Progress Report No. 42-109, 1992, pp. 40–55.
[15] D.E. Lebach *et al.*, Phys. Rev. Lett. **75**, 1439 (1995).
[16] J.M. Longuski, R.E. Todd, and W.W. König, J. Guid. Control Dyn. **15**, 545 (1992).
[17] C.W.F. Everitt and S. Buchman, in *Particle Astrophysics, Atomic Physics, and Gravitation*, edited by J. Trân Thanh Vân, G. Fontaine, and E. Hinds (Editions Frontières, Gif-sur-Yvette, 1994), p. 467.
[18] STEP Testing the Equivalence Principle in Space Proceedings, Pisa, 1993, edited by R. Reinhard.
[19] A.M. Nobili *et al.*, J. Astronaut. Sci. **43**, 219 (1995).
[20] O. Montenbruck and E. Gill, *Satellite Orbits* (Springer-Verlag, New York, 2001).
[21] J. Prussing and B. Conway, *Orbital Mechanics* (Oxford University Press, New York, 1993).
[22] S.W. Thurman and C.B. Sybert, Adv. Astronaut. Sci. **76**, 1039 (1992).
[23] T.W. Hamilton and W.G. Melbourne, JPL Space Programs Summary 3, No. 37–39, 1966, pp. 18–23.
[24] R.A. Brouke, Astron. Astrophys. **6**, 173 (1970).
[25] K. Vulkov, J. Br. Interplanet. Soc. **31**, 111 (1978).